Spring 2013

Parameter optimization for controlling aluminum loss when laser depositing Ti-6Al-4V

Richard Charles Barclay

Department:

PARAMETER OPTIMIZATION FOR CONTROLLING ALUMINUM LOSS WHEN LASER DEPOSITING Ti-6Al-4V

by

RICHARD CHARLES BARCLAY

A THESIS

Presented to the Faculty of the Graduate School of the

MISSOURI UNIVERSITY OF SCIENCE AND TECHNOLOGY

In Partial Fulfillment of the Requirements for the Degree

MASTER OF SCIENCE IN MANUFACTURING ENGINEERING

2013

Approved by:

Dr. Frank Liou, Advisor

Dr. Joseph W. Newkirk

Dr. Elizabeth A. Cudney

ABSTRACT

The ability to predict the mechanical properties of engineering materials is crucial to the manufacturing of advanced products. In the aerospace industry, Ti-6Al-4V is commonly used to build structures. Any deviation from the alloy's standard properties can prove detrimental. Thus, the compositional integrity of the material must be controlled.

The ability to directly build and repair large, complicated structures directly from CAD files is highly sought after. Laser Metal Deposition (LMD) technology has the potential to deliver that ability. Before this process can gain widespread acceptance, however, a set of process parameters must be established that yield finished parts of consistent chemical composition. This research aims to establish such a set of parameters.

Design of Experiments was utilized to maximize the information gained while minimizing the number of experimental trials required. A randomized, two-factor experiment was designed, performed, and replicated. Another set of experiments (nearly identical to the first) was then performed. The first set of experiments was completed in an open environment, while the second set was performed in an argon chamber. Energy Dispersive X-Ray Spectroscopy (EDS) was then used to perform a quantitative microanalysis to determine the aluminum level in each sample. Regression analysis was performed on the results to determine the factors of importance. Finally, fit plots and response surface curves were used to determine an optimal parameter set (process window). The process window was established to allow for consistent chemical composition of laser deposited Ti64 parts.

ACKNOWLEDGEMENTS

Rarely can one complete an investigation spanning multiple engineering disciplines without receiving help, guidance, and support from others. This research was no exception. While the true list of all I owe thanks to is very large, I must focus here on those most influential to this project. I would like to begin by thanking my advisor, Dr. Frank Liou, for his generous support and guidance over the past two years. I would also like to thank the manufacturing engineering department for the research assistantship provided to me.

I am grateful to Todd Sparks for both his input and guidance throughout the entire course of this work. I must thank Yu-Herng Pan for his assistance in performing the experiments. I would like to thank my committee members, Dr. Joseph Newkirk and Dr. Elizabeth Cudney, for their input and guidance along the way. I would also like to thank all of those associated with the LAMP Lab at Missouri University of Science and Technology for the support and memories provided over the past two years.

Finally, I would like to thank my parents, Rich and Sue Barclay, as well as my sisters Kristi, Karena, and Kelli, for their unwavering love and support. Thank you for always believing in me, even when I did not believe in myself.

TABLE OF CONTENTS

Page

LIST OF ILLUSTRATIONS

Page

LIST OF TABLES

Page

1. INTRODUCTION

1.1. OVERVIEW

Laser Metal Deposition (LMD) shows great promise for directly producing metal parts from Computer Aided Design (CAD) files [1]. LMD has the potential to produce parts which are fully dense and net shape [2]. Many industries have seen the potential impact of LMD technology in their respective fields. One of these industries is the aerospace industry. Within this industry, large titanium structures are often manufactured and used in the production of air vehicle platforms. The ability to directly manufacture and repair these structures could greatly reduce both the time and cost normally associated with current aerospace manufacturing practices.

The most common aerospace structural titanium alloy is Ti-6Al-4V (Ti64) [3]. If any manufacturing process is to gain widespread acceptance and commercialization within the aerospace industry, it must have well-known, documented processing parameters for Ti64. The parameters must be able to produce parts with sufficient dimensional accuracy, surface finish, and aesthetic qualities. However, the process must also be able to produce parts with proper chemical composition.

The occurrence of chemistry changes in materials during processing is not a new concept. One of the more common manufacturing processes is casting. In the casting process material is heated until it transitions to a liquid state. Once the material has reached a liquid state, it is poured into a mold and allowed to solidify. During the casting of metals, it has been found that holding an alloy at a liquid state for extended periods of

time can result in a reduction in the percentage of various elements within an alloy. This phenomenon is known as ‘fading’. The effect of fading in casting of different alloys is well known [4][5]. There are several potential causes of fade loss in castings. The losses could be the result of elements settling during the holding period. The losses could also be caused by oxidation of elements which in turn could rise to the surface of the casting as slag. A third potential cause could be evaporation. Regardless of the mechanism for loss, the losses have been established in previous work.

Another process which induces changes in material composition during processing is electron beam welding. Electron beam welding has gained a lot of popularity for its ability to produce very narrow, deep penetration welds. These deep penetration welds are produced by the electron beam’s ability to produce a cavity or ‘keyhole’ in the material to be welded. This cavity is formed, and maintained by the vaporization of metal [6]. This vaporization of metal is not only known, but is a necessity for the process. The fact that these losses are occurring lends to the idea of changes in chemical composition. The vaporization of elements within an alloy are likely to occur at different rates. This fact is what leads to the idea of compositional changes. The idea of elements vaporizing at different rates, or preferential vaporization, will be discussed in the following paragraphs.

The nature of many thermal processes is such that they can induce preferential vaporization when depositing certain alloys. Ti64 is one alloy which has experienced these losses during processing. Ti64 has been shown to lose between 10 wt% and 15 wt% of the original aluminum content during electron beam (Ebeam) deposition processes [3]. This preferential vaporization is due to the fact that aluminum has a high vapor pressure

with respect to titanium and vanadium [3]. Vapor pressure is an important factor with Ebeam deposition since the process is performed in a vacuum. With the reduced pressure experienced in a vacuum, the temperature at which the element will transition from liquid to gas is lowered. This is analogous to cooking at high altitudes, where the atmospheric pressure is lower, water boils at a lower temperature. This lower temperature makes it more difficult to cook food since the water, and food, don't get as hot as they would at lower altitude (and lower pressure).

The focus of this work, LMD, is similar in concept to Ebeam deposition and both processes are analogous to welding. In welding processes a heat source is used to heat a plate, creating a melt pool. Filler metal is then added to the melt pool to create a weld bead. Ebeam deposition and LMD both use a heat source to heat a plate and create a melt pool. Both processes also add filler metal to the melt pool to build parts. Although both processes use a heat source and add filler metal, the heat sources are considerably different. Ebeam deposition uses a high power, focused electron beam to heat the substrate. The nature of the electron beam is such that it acts to 'drill' a hole in the substrate, creating a relatively large interaction volume, and vaporizing material in the process. LMD systems use a high power laser to provide the heat source. The laser tends to act primarily on the surface of the substrate, penetrating to a depth of a few nanometers.

An additional difference between Ebeam deposition and LMD lies in the processing environment. As mentioned previously, Ebeam deposition occurs inside of a vacuum chamber. LMD however, occurs in an inert environment at atmospheric pressure. And, as mentioned earlier, the reduced pressure in a vacuum would lower the temperature

at which the aluminum would begin to vaporize. Conversely, since LMD is performed at atmospheric pressure, the temperature required to vaporize aluminum would be higher.

The differences mentioned above could cause Ebeam and LMD processes to behave differently with regard to evaporative losses. Additionally, the fading losses which occur in casting, which were discussed previously, while not directly applicable to the LMD process, do serve to illustrate the effects that can be caused by holding an element in its liquid state for extended periods of time. A major difference between holding in casting and the LMD process is the time in which the material is held in its liquid state. The hold time in the casting studies mentioned earlier, ranged from several minutes to several hours. In LMD however, the time in which the metal is held in its liquid state is on the order of milliseconds.

The purpose of the discussion to this point has been to illustrate the fact that other, similar manufacturing processes experience chemical losses during processing. The mechanism for the losses may be different, and as pointed out in the previous discussion there are major inherent differences between the processes. However, the fact that these losses occur in similar processes is the basis for this work. Although it is believed that LMD processes will experience some aluminum loss during processing. It is not known to what extent the losses occur, or if there is any measurable loss at all.

The belief that the LMD process likely experiences some aluminum loss during processing is based upon a couple of factors. The first factor is one that was discussed at length previously; the fact that other similar processes experience losses through various mechanisms. Another factor is due to observations that have been made during previous

LMD processing. It has been noticed that while depositing different alloys, Ti64 included, an oxide layer appears on equipment and tends to coat the inside of the deposition chamber. It is believed that this oxide layer may be due to elements oxidizing during the process and escaping from solution.

These before mentioned losses are likely the result of extremely high temperatures experienced during the deposition process. As mentioned earlier, vapor pressure has been linked to evaporative losses in Ebeam deposition. At atmospheric pressure pure elements will tend to evaporate at their boiling point, since at that temperature the vapor pressure is equal to the atmospheric pressure. However, when considering alloys the relationship becomes much more complicated. The temperature required for the element to separate from solution and escape into the atmosphere through vaporization is likely much higher. Table 1.1 lists the alloying elements of Ti64 and their respective melting and boiling points [7][8][9][10].

Table 1.1. Melting and boiling points of Ti64 alloying elements.

Element	Melting Point (°C)	Boiling Point (°C)
Titanium	1668	3287
Aluminum	660.3	2520
Vanadium	1910	3407
Ti64	1604-1660	

During the LMD process, the temperatures often hover between 2000° C - 2200° C. The fact that the peak process temperature remains at a high level throughout the

course of deposition is believed to accelerate the evaporative losses. These evaporative losses are what this work seeks to minimize. Changes in the chemical makeup created by these conditions can adversely affect both the mechanical properties of the alloy and the structures created from it. These changes can be detrimental to the integrity of the structures [3]. Figure 1.1 illustrates the temperature dependence on the rate of evaporation of aluminum, titanium, and vanadium from liquid Ti-6Al-4V. This figure was created through the construction of a model. This model was based on not only the Langmuir equation but also thermodynamic estimates of the activity coefficients [11]. This illustration is meant to provide a visual representation of the evaporation rates of titanium (Ti), aluminum (Al), and vanadium (V).

In order to prevent the adverse effects caused by a change in chemistry, it is imperative to determine a set, or a range, of optimal process parameters (process window). This process window will allow for minimization of aluminum loss, and mitigate the risk inherent with such losses. The purpose of this research was to investigate the relationship between two key LMD process parameters and the resulting aluminum content of the deposit. Both energy and feed rate were the investigated parameters. Energy was measured per unit length in Joules per millimeter (J/mm). The feed rate was measured in millimeters per minute (mm/min). The ability to relate these parameters to aluminum loss is paramount for the future commercialization of the LMD process. Establishing this relationship will help create structures of acceptable chemical makeup. Additionally, quantifying these relationships will help in the development of analytical models used to simulate LMD processes. These models will aid in predicting

the composition of deposits. These predictions could prove very useful in the design and process planning stages of product development.

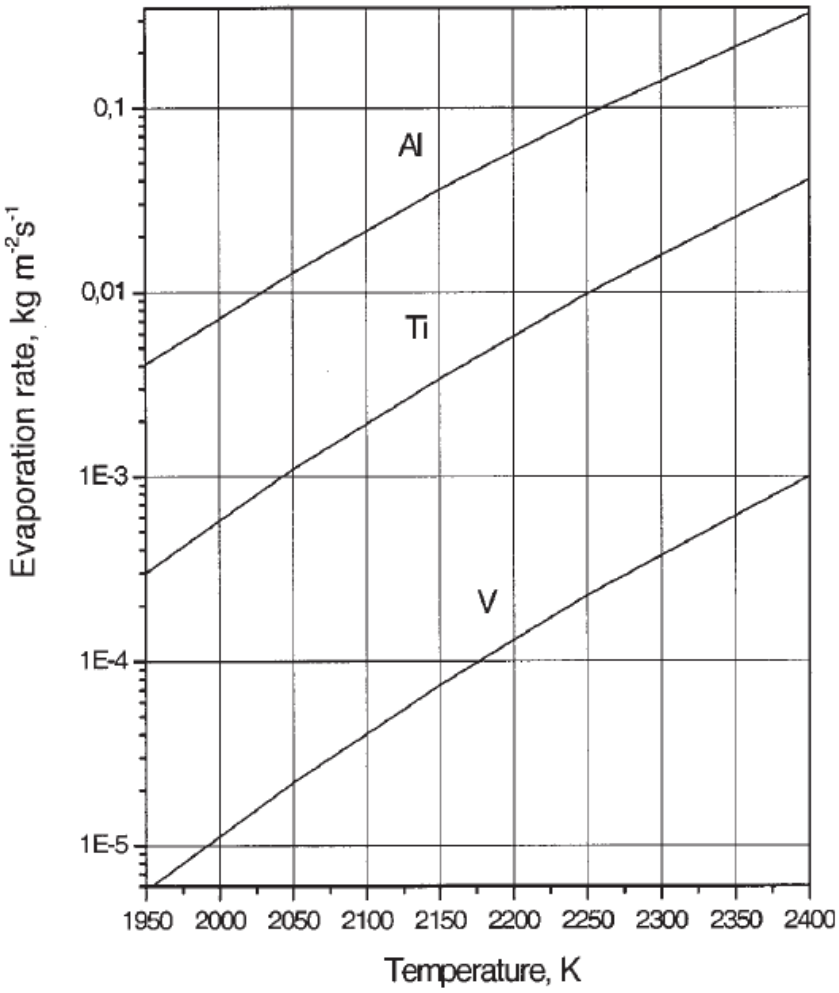

Figure 1.1. Evaporation rates of Ti64 alloying elements.

Design of Experiments (DoE) was employed to identify the critical process parameters. The experiment was then performed in the Laser Aided Manufacturing Process (LAMP) Lab at Missouri University of Science and Technology (Missouri S&T). This study utilized the 1 kW Nuvonyx Diode Laser in the LAMP Lab. After the experiment was conducted, x-ray microanalysis was performed on the specimen to quantify the amount of aluminum present in the samples. After the microanalysis was completed, a regression analysis was performed on the results generating fit plots and response surface curves for optimal parameter set identification

1.2. LASER METAL DEPOSITION

Blown Powder Laser Metal Deposition (LMD) is a process in which a laser is used to heat a substrate. Metal powder particles are then blown into the melt pool. This process is normally completed in a continuous manner, with many layers being deposited on top of each other to create a fully dense structure [12]. Figure 1.2 depicts a generic LMD system. The direction of travel indicated in the figure corresponds with the traverse feed rate factor investigated in this research. The energy factor (which was investigated) is represented by the laser beam (depicted in the figure). The powder particles are representative of the powder flow rate (described in the following section). Figure 1.3 is a generic representation of the LMD system in use in the LAMP Lab at Missouri S&T, and Figure 1.4 is an image of the actual LMD system used for this experiment in the LAMP Lab.

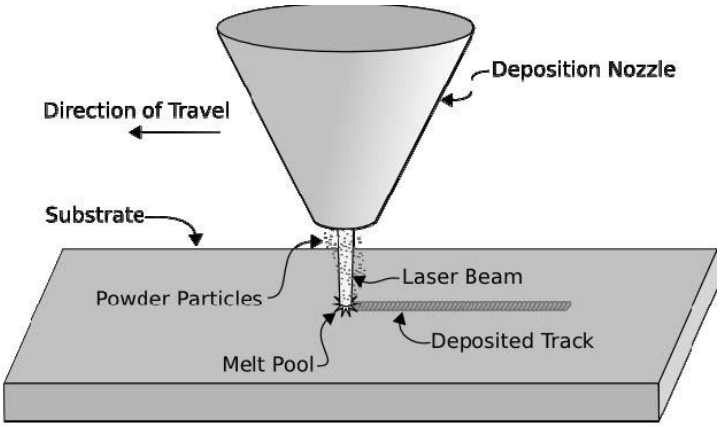

Figure 1.2. Generic Representation of a LMD System [13].

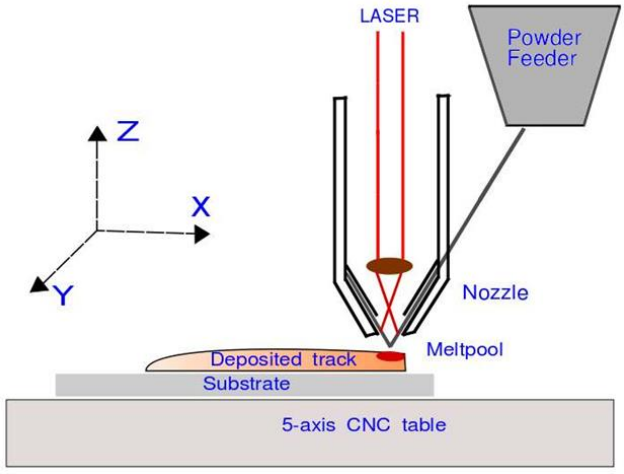

Figure 1.3. Generic Representation of LAMP Lab's LMD System.

Figure 1.4. LAMP Lab's LMD System.

Work has been done to establish a process window in which Ebeam deposition can be efficiently performed to minimize or control aluminum loss [3]. However, no published work could be found by the author of this work, detailing the establishment of a process window for laser deposition of Ti64. This work seeks to make an original contribution to the field of advanced manufacturing. In particular, a process window which will allow for optimized laser deposition of Ti-6Al-4V will be established.

2. EXPERIMENTAL PROCEDURE

2.1. DESIGN OF EXPERIMENTS

One must understand the cause and effect relationships between both the inputs to the process and the outputs from the process to fully understand the way that process works. For this to occur, one must observe the process while intentionally changing the inputs to observe the changes in output. From these observations, an empirical model can be created to define the process [14]. Design of Experiments (DoE) is a methodical approach by which to accomplish this in an efficient manner. DoE allows for efficient planning and conducting of experiments. Additionally, DoE provides tools for analyzing the resulting data so that valid and objective conclusions are obtained [14].

A two-level, two-factor design was chosen for this research. A midpoint was also used to check for linearity. For the purpose of this work, the variables of energy and traverse feed rate were considered to be the most likely factors affecting the aluminum content of the deposits. Therefore, these two variables were chosen as the design factors to be varied. Another variable encountered in LMD is powder flow rate. This was negated by varying the powder flow rate proportionally to the feed rate so that the total amount of powder blown into the deposit remained approximately constant.

It was deemed important to be able to apply the results of this work across a wide scope of Ti64 deposits with varying geometries. The experimental factors were selected in such a way as to reduce the effects imposed by varying geometries. While this is impossible to do in reality, it was important to consider while designing the experiment.

Thus, the factor of energy was selected in terms of energy per unit length of linear deposit, or J/mm. Observing the effect of energy in this manner was the best way to gain results less dependent upon geometry.

Table 2.1 represents the experimental design constructed for the purpose of this work. As previously mentioned, the selected design called for high-low combinations with a center point. This design resulted in the four corners and center point in Table 2.1.

Table 2.1. Experimental Parameter Sets.

		Energy (J/mm)		
		85	97.5	110
Feed (mm/min)	375	X		X
	455		X	
	535	X		X

2.2. EXPERIMENTAL SETUP

The experiments performed in the course of this work were completed on a LMD system consisting of the following:

- 1.0 kW Nuvonyx Diode Laser
- Bay State Technologies Model 1200 Powder Feeder
- Precitec YC50 Cladding Head
- National Instruments PXI-8195-RT Real Time Controller

The equipment is part of the LAMP Lab at Missouri S&T.

These experiments were performed in two blocks due to the different deposition environments available at Missouri S&T. The standard deposition environment for Ti64 (at Missouri S&T) is inside an argon chamber. It was determined that the best, most cost-effective method for accomplishing this chamber was with turkey bags. These bags are the standard bags used in households to cook turkeys. They attach easily both to the base of the CNC table and to the top of the laser nozzle, creating a quick, flexible, easy to change/repair, cost-effective argon chamber in which to perform deposition.

Figure 2.1 is a photo of an experiment being performed inside a turkey bag. The metal shroud surrounding the nozzle helped to protect the bag from powder particles that might bounce off of the melt pool. The waves (running from the top of the picture towards the bottom), just to the left of center, are reflections of light off of the turkey bag. These waves are caused by wrinkles in the bag.

The other deposition environment (and experimental block) used in this work was an argon flood (through an aluminum shroud). This method involved placing an aluminum shroud around the laser nozzle. The shroud accepted gas fittings on the top, allowing argon to be pumped into the shroud. The argon was then expelled through the bottom of the shroud, flooding the build area with argon gas. This method devoured large amounts of argon. Depending upon the geometry to be deposited this method is sometimes necessary.

Figure 2.2 is a photo of deposition being performed with the shroud attached. The white hoses attached to the top of the shroud are the argon gas feeder lines.

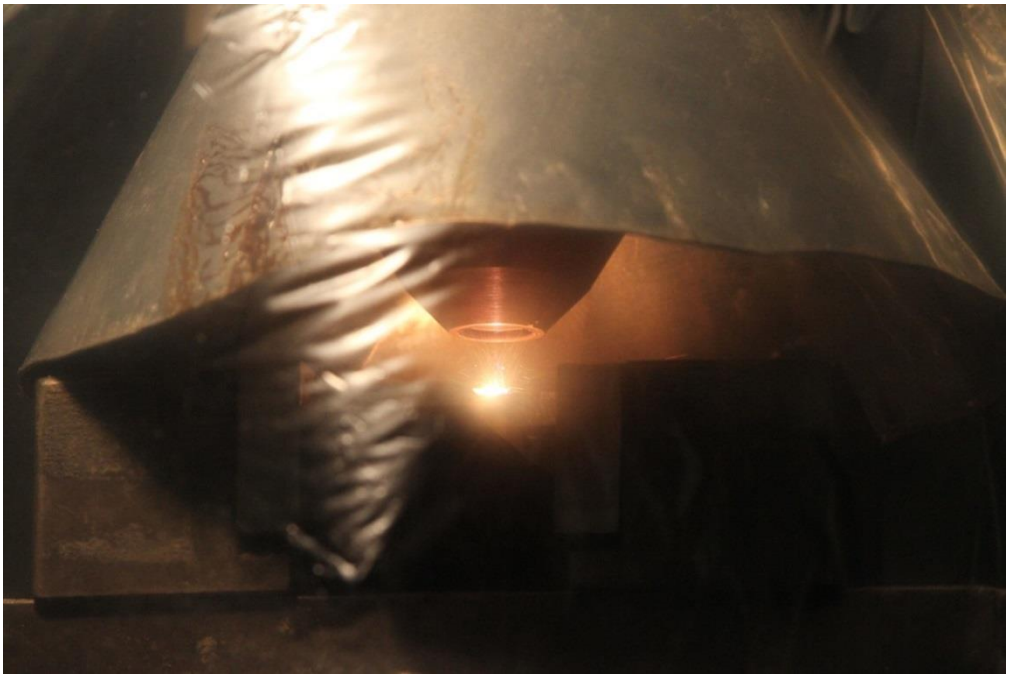

Figure 2.1. Deposition inside of a turkey bag.

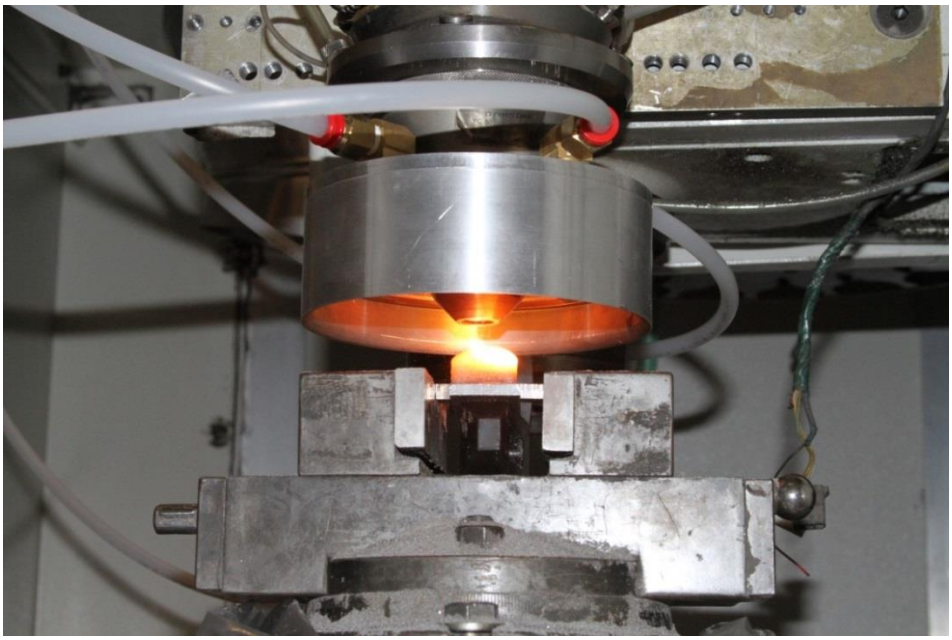

Figure 2.2. Deposition being performed with the shroud attached.

2.3. EXPERIMENTAL DEPOSITION

The metal powder used for this experiment was a Ti-6Al-4V (Ti64) alloy with a size distribution of -60 +120 mesh. The powder was deposited onto Ti64 plates (substrates) measuring approximately 0.5” x 2.0”. The substrates were all engraved with a unique ID number, from 1 to 22, to allow for easy tracking during processing and analysis. The deposition for this experiment was performed for one day. All deposits were thin walls (the width of the deposit consisted of a single track). A total of 50 layers were deposited on each substrate. Each layer was approximately 320 μm thick and 25 mm in length. As mentioned in section 2.1, the total amount of powder delivered to the deposit was held constant at approximately 24.13 g. This was accomplished by varying the powder flow rate proportionally to the traverse feed rate. Subsequently delivering an amount of powder that was equal per unit length, over all deposits.

2.3.1. Deposition with a Turkey Bag. All of the experimental runs using the turkey bag were completed first. The first deposit was attempted on substrate 1. The deposit failed, however, due to a misalignment of the laser nozzle. This was corrected, and the first deposit was repeated on substrate 21. The remaining turkey bag deposits (2-10) were completed without incident.

Figure 2.3 is deposit 2 after completion. Table 2.2 lists the run-order corresponding to each substrate number and parameter set. This list covers all deposits completed with the turkey bag.

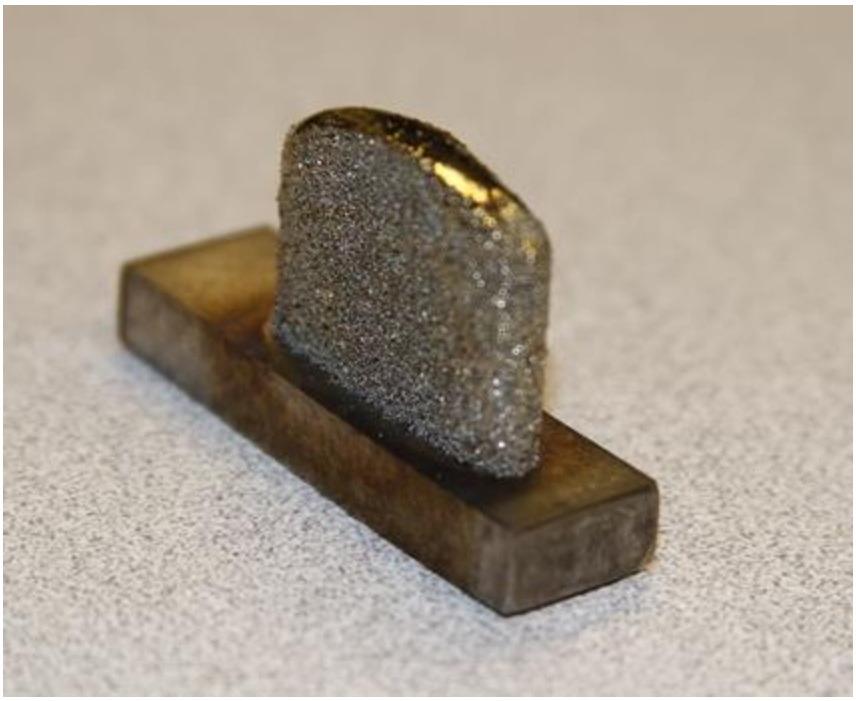

Figure 2.3. Deposit performed on substrate 2.

Table 2.2. Experimental run order for the turkey bag.

Run Order	Substrate #	E (J/mm)	F (mm/min)	M (g/min) [Ti]
1	21	97.5	455	8.78
2	2	110	375	7.24
3	3	110	535	10.33
4	4	97.5	455	8.78
5	5	110	375	7.24
6	6	85	535	10.33
7	7	85	375	7.24
8	8	110	535	10.33
9	9	85	375	7.24
10	10	85	535	10.33

2.3.2. Deposition with a Shroud. After the turkey bag deposits were completed, the shroud deposits were run. The shroud deposits began with run 11 and proceeded without problems until run 18. During run 18, the powder feeder ran out of powder, causing the build to fail. The powder feeder was reloaded with powder, and run 18 was repeated successfully on substrate 22. The remaining deposits (19 and 20) were completed without issue. Figure 2.4 is deposit 11 after completion. Table 2.3 lists the run-order of each shroud substrate with the corresponding parameter set.

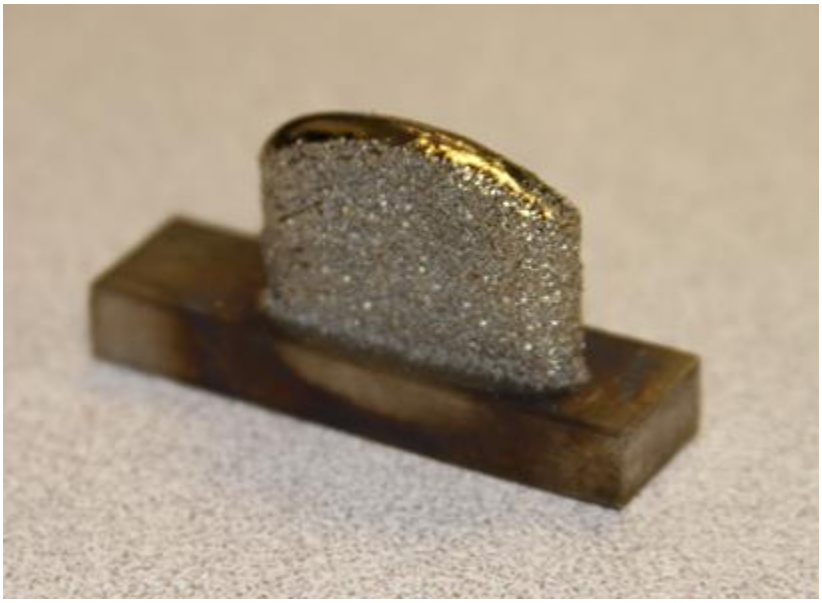

Figure 2.4. Deposit performed on substrate 11.

Table 2.3. Experimental run order for the shroud.

Run Order	Substrate #	E (J/mm)	F (mm/min)	M (g/min) [Ti]
11	11	97.5	455	8.78
12	12	110	375	7.24
13	13	110	535	10.33
14	14	97.5	455	8.78
15	15	110	375	7.24
16	16	85	535	10.33
17	17	85	375	7.24
18	22	110	535	10.33
19	19	85	375	7.24
20	20	85	535	10.33

3. QUANTITATIVE MICROANALYSIS

Energy Dispersive X-Ray Spectroscopy (EDS) was performed to quantify the amount of aluminum present in each deposit. The samples were prepared for analysis using standard metallographic techniques. A matrix of measurements was then taken at different points on each deposit. A total of 70 data points were collected over the 20 samples. This portion of the research was conducted in the Advanced Material Characterization Lab (AMCL) at Missouri S&T.

3.1. SAMPLE PREPARATION

3.1.1. Machining of Deposits. The deposits were first machined to a more manageable size to reduce the time spent polishing samples. The deposits were machined along the long axis until reaching a point just before the apparent center point of the short axis. Two cuts were then made with a saw, each approximately ¼" from the center of the deposit. These cuts ran from the top of the deposit to the substrate, creating a section approximately ½" wide. The deposit was then removed from the substrate with a final saw cut, freeing both the ½" coupon (test section) and the remainder of the deposit.

After the deposit was removed, the substrate, the coupon, and the remainder of the deposit were all placed into individual storage devices allowing for easy identification and separation of coupons throughout the course of the work.

Figure 3.1 is a diagram of the coupon section to be removed from substrate 2. The X axis corresponds to the long axis, the Y axis corresponds to the short axis, and the hatched section in the middle is where the coupon was taken from.

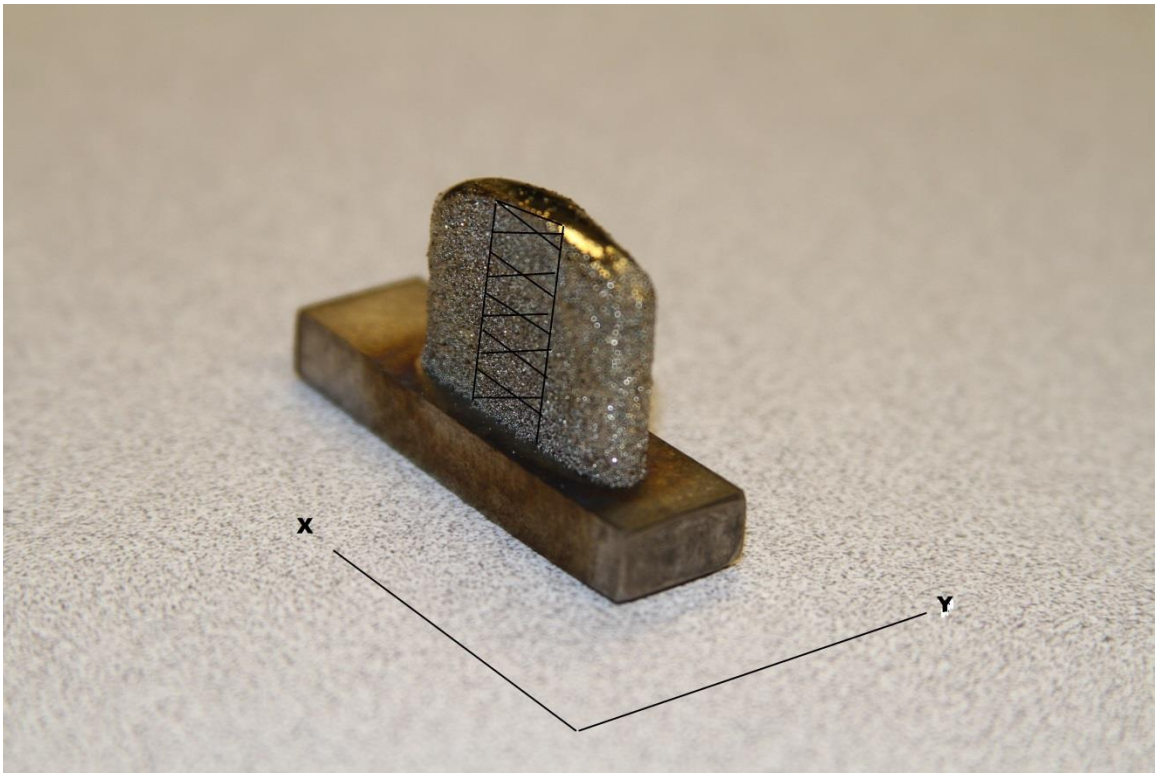

Figure 3.1. Schematic of the coupon section to be removed from the deposit made on substrate 2. The hatched section represents the coupon section.

3.1.2. Polishing of Coupons. After machining was complete, the coupons were polished to a mirror finish. This polishing was necessary to perform EDS analysis; EDS works best when the surface to be analyzed is completely flat and free of scratches. Polishing was performed on an automatic rotary polisher and the polishing consisted of

two phases: grinding and polishing. The first phase involved the use of Silicon Carbide (SiC) abrasives. The SiC grit size ranged from 120 to 1200, with the smaller grit being the more abrasive and first used. Table 3.1 shows the entire schedule used to grind the coupons.

Table 3.1. Grinding schedule for Ti64 coupons.

GRINDING	SiC Grit Size	Time (s)	Wheel Speed (RPM)	Pressure (psi)
1	120	180	300	40
2	240	180	300	40
3	400	180	300	40
4	600	180	300	40
5	800	180	300	40
6	1200	180	300	40

After grinding was complete, the coupons were polished to a mirror finish. This was completed with polishing compounds. These compounds were applied to a polishing cloth mounted in the automatic polisher. Two different polishing compounds were used, sequentially. Table 3.2 details the entire polishing schedule that was followed in the final polishing. Figures 3.2 and 3.3 show coupon 21 after polishing. Note the reflection in Figure 3.3 of the camera lens and flashbulb, indicating a mirror finish on the coupon.

Table 3.2. Polishing schedule for Ti64 deposits.

POLISHING	Polishing Compound	Time (s)	Wheel Speed (RPM)	Pressure (psi)
1	9MM	300	250	30
2	Colloidal Silica	300	150	15

Figure 3.2. Coupon 21 after polishing.

Figure 3.3. Coupon 21 after polishing. Note the reflection of the camera lens and flash bulb, indicating a mirror finish.

3.2. ENERGY DISPERSIVE X-RAY SPECTROSCOPY (EDS)

The quantitative analysis for this work was completed on an FEI Helios NanoLab 600 Scanning Electron Microscope (SEM). The scope was equipped with an EDS gun producing a 50 mm spot size. A standard-based quantitative analysis was performed. The standard-based analysis was chosen because it can produce a higher degree of certainty. This standard was purchased from an outside vendor. The scope was calibrated immediately before any measurements were taken. This calibration was completed with the standard and the accompanying compositional specifications (provided by the vendor).

The analysis was run over the course of several days. In order to better determine where to take measurements from when in the SEM, a series of lines were drawn on the coupons with a Sharpie pen. The lines denoted the center section of the coupon as well as the bottom, middle, and top. Three to five coupons were mounted onto a sample holder, along with the standard, and then loaded into the SEM. The SEM was then focused and stigmated. The initial calibration using the standard was then completed. Once calibration was complete, the coupons were located, one at a time, and a series of measurements was taken. These measurements were taken along the centerline of the coupon at three locations: bottom (B), middle (M), and top (T). Bottom corresponds to the section that was attached to the substrate initially. This process was repeated for all 20 deposits. The parameters used for the EDS analysis were as follows:

- Accelerating Voltage = 15 kV
- Beam Current = 1.4 nA
- Working Distance = 4 mm
- Process Time = 2 sec
- Live Time = 100 sec

The normalization routine forces the weight percent of all elements considered in the EDS analysis to total 100%. This routine can skew the results by adding an additional weight percent that is not really present. Thus, the normalization was turned off.

The EDS analysis was conducted without issue. A total of 70 data points was collected. Figure 3.4 is the SEM (and related hardware) that was used to complete this work.

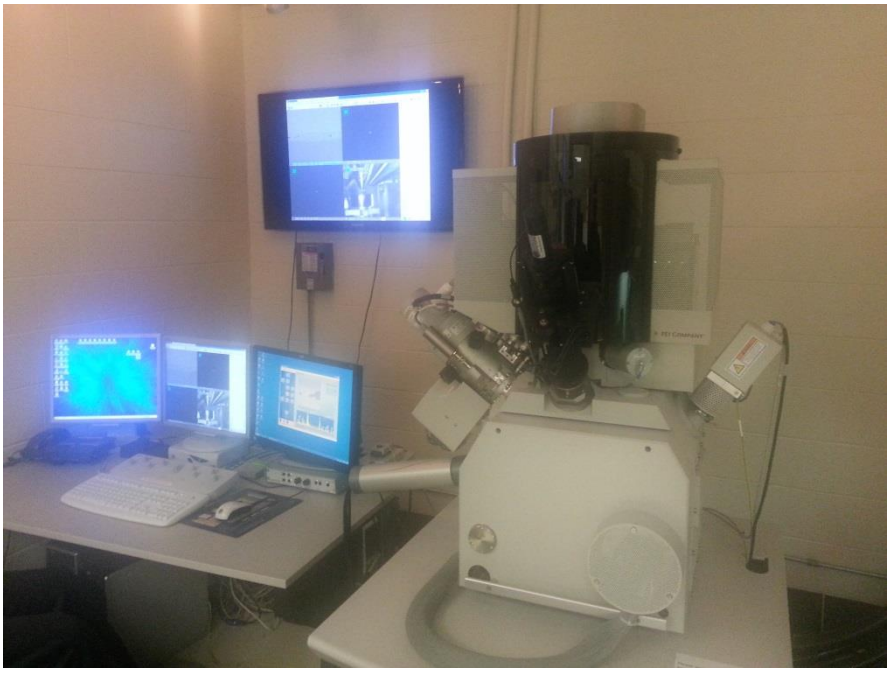

Figure 3.4. SEM housed in the AMCL at Missouri S&T.

4. RESULTS AND DISCUSSION

The data produced by the EDS analysis was gathered into an excel file, allowing the data to be easily organized. During analysis, the average aluminum levels were found to be near what one might expect them to be (6.08 %). Considerable variation did exist, however, among the deposits. Occasionally even among different locations (sometimes different locations very close to one another) on the same deposit. This finding was to be expected, as this variation was the focus of this study. In addition, the variation within a deposit was also investigated to see if there is any correlation between location within the deposit, and aluminum content.

The statistical analysis for this work was performed in SAS (Statistical Analysis Software). Two different statistical models were built during this analysis. The main model was built to test for the main effects of energy and feedrate, the interaction between the two, blocking effect (turkey bag, shroud), and location (of the measurement, B, M, T). A secondary model was built to test for run order effects. This was done to account for any drift that may have occurred during the deposition process. It was necessary to build a separate run order model due to the number of degrees of freedom required for the analysis. The blocking effect was examined to determine whether or not any statistical significance tied the method of the deposit (turkey bag or shroud) to the resulting aluminum content. The location was checked to see if there was any significant difference in aluminum content based upon the location in the deposit (Bottom, Middle, and Top). Run order was tested separately to account for any variability in the machine and the significance of any system drift on aluminum content.

The secondary model did show some significance tied to the run order. Since the run order was completely randomized, this was likely due to the deposition system drifting throughout the process. Drifting can be the result of misalignments which progressively get worse throughout the course of several deposits. This progression often leads to subtle changes in powder delivery and energy input to the deposit. While there was a slight significance tied to this factor, it was minimal when compared to the main effects of energy and feedrate. For that reason it was removed from the model to allow for a more detailed examination of the experimental variables.

The main statistical model built for data analysis consisted of two blocks: turkey bag, and shroud. This model tested two experimental variables (Energy and Feedrate) and examined the aluminum levels at different locations along the deposit. One response variable (aluminum content) was considered. Table 4.1 lists both the class and level information for the experiment. Additionally, the total number of observations is shown.

Table 4.1. Class level information for the statistical model.

Class	Levels	Values
block	2	shroud turkeybag
location	3	b m t
energy	3	85 97.5 110
feedrate	3	375 455 535
Number of Observations Read		70
Number of Observations Used		70

Table 4.2 lists the overall ANOVA for this experiment. Notice the ‘P’ value in the far right column. This number represents the significance level of the experiment. In general, a significance level of 0.05 or smaller, indicates that the model has a very small chance to produce a Type 1 error. The ‘P’ value (shown below) 0.0023 corresponds to a confidence level of 99.77%. This value indicates a high level of confidence in the statistical model created for this work.

Table 4.2. Overall ANOVA for the statistical analysis.

Source	DF	Sum of Squares	Mean Square	F Value	Pr > F
Model	7	6.52404756	0.93200679	3.66	0.0023
Error	62	15.76992958	0.2543537		
Corrected Total	69	22.29397714			

The data that was used in this statistical model was unbalanced (there weren’t an equal number of observations for all treatment combinations). Therefore, a Type III Sum of Squares (SS) was used to analyze the results of this model. In addition to the main effects of energy and feedrate, the interaction between the two was also included. Table 4.3 lists the results of the ANOVA. When reading an ANOVA table for an experiment with interactions, the first effect to test is the interaction effect. Note the ‘P’ value (shown below) for the interaction between energy and feedrate (energy*feedrate) in the table. As a general rule of thumb if the ‘P’ value (significance level) is less than or equal to 0.05 then the interaction effect is very significant and the main effects involved in the interaction need not be tested individually. The ‘P’ value (shown below) 0.0008 is nearly

two orders of magnitude lower than the rule of thumb. Therefore, it can be stated that the interaction effect between energy and feedrate is very statistically significant. This interaction effect is instrumental in controlling the final aluminum content of Ti64 deposits made using the LMD system in the LAMP Lab.

Experimental block and deposit location were evaluated in addition to energy and feedrate. As shown in Table 4.3, the significance level for both block and location is very high (0.6609 and 0.467, respectively) indicating that there is no statistical significance between either of these factors and the resulting aluminum content in the deposits.

Table 4.3. Type III ANOVA for the statistical model built for this experiment.

Source	DF	Type III SS	Mean Square	F Value	Pr > F
block	1	0.04940467	0.04940467	0.19	0.6609
location	2	0.39208508	0.19604254	0.77	0.467
energy	1	0.13041889	0.13041889	0.51	0.4766
feedrate	1	1.19169442	1.19169442	4.69	0.0343
energy*feedrate	1	3.13654547	3.13654547	12.33	0.0008

Upon completing the statistical analysis, it was necessary to examine the results further in order to establish an optimal parameter set. The word “optimize” can be very subjective, and is definitely relative. Therefore, it was determined that for this work an optimized solution set should consist of a range of process parameters (process window) which would allow for consistent chemical composition across deposits. This was

deemed optimal because consistent mechanical properties is a critical characteristic of any engineering material, and especially critical in aerospace structures.

To determine an optimal solution set, response surface plots were created. The surface plots used in this work were created using spline interpolation. Spline interpolation allows for smoothing of graphs by filling in missing data points through interpolation. Figures 4.1 and 4.2 are the response surface plots that were created for the entire data set. Figure 4.1 is displayed using SAS default settings of 45° rotation, and 70° tilt. Figure 4.2 is shown with 135° rotation and 80° tilt.

Notice the flat region in Figure 4.1, beginning at the top left corner and extending towards the middle. This region shows a band of parameter sets which produce deposits of consistent aluminum content. Figure 4.2 shows the region from a different angle, allowing for easy visualization of the optimal solution set.

The results shown in the figures below were very surprising. Conventional thinking dictates that as energy increases, feedrate must increase as well. This should help limit excess heat input into the build and prevent accelerated aluminum vaporization. The figures (shown below) indicate that, in fact, a slower, hotter build produces deposits with higher aluminum content.

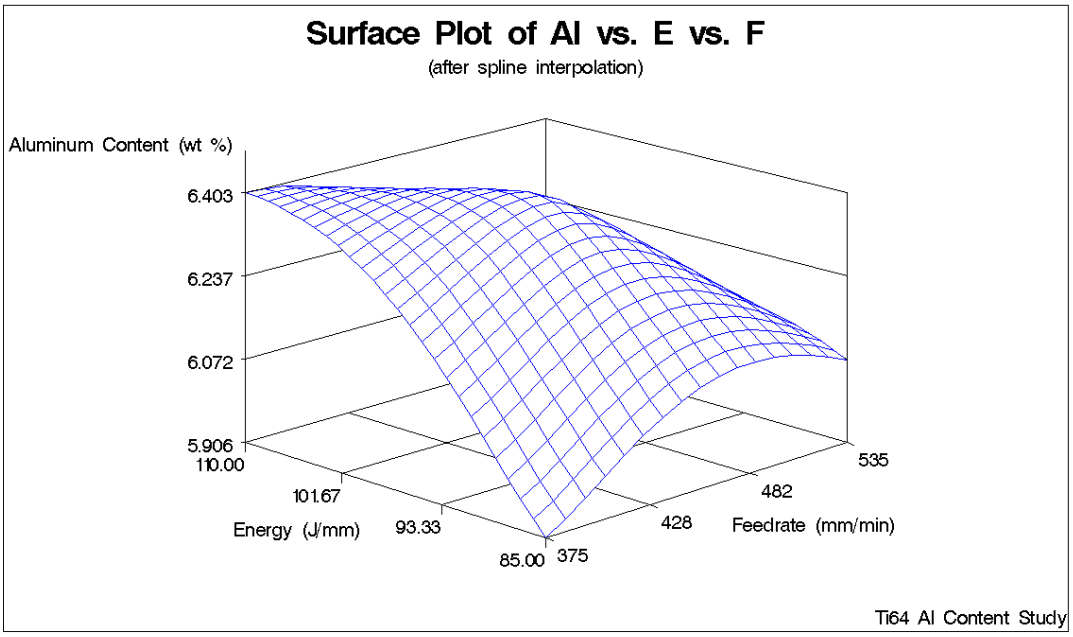

Figure 4.1. Response surface plot of entire data set, shown with default rotation and tilt.

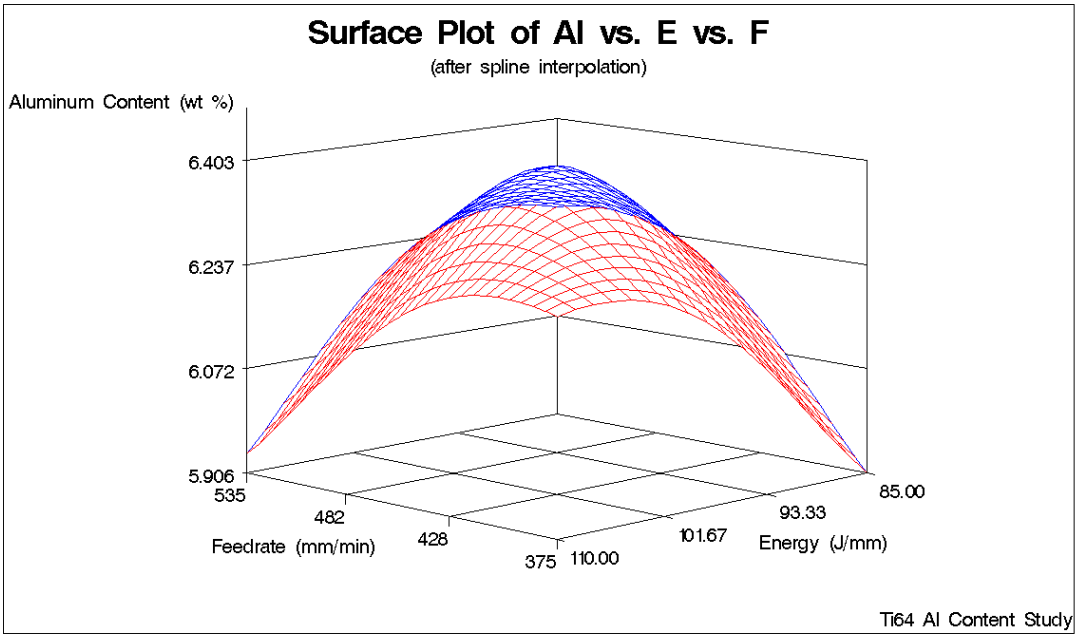

Figure 4.2. Surface plot of entire data set, shown with 135° rotation, and 80° tilt.

In order to further investigate potential solution sets, additional surface plots were created using just the turkey bag data, and just the shroud data. Surface plots of the turkey bag data are shown in Figures 4.3 and 4.4. Notice the flat spot in the top left corner of Figure 4.3. Figure 4.4 shows the same graph but with a 135° rotation and 80° tilt.

In both of the turkey bag plots (shown below), a flat surface exists in which the optimal solution set resides. It is noted that the solution set for the turkey bag data is slightly larger and flatter than the overall solution set generated for the entire data set.

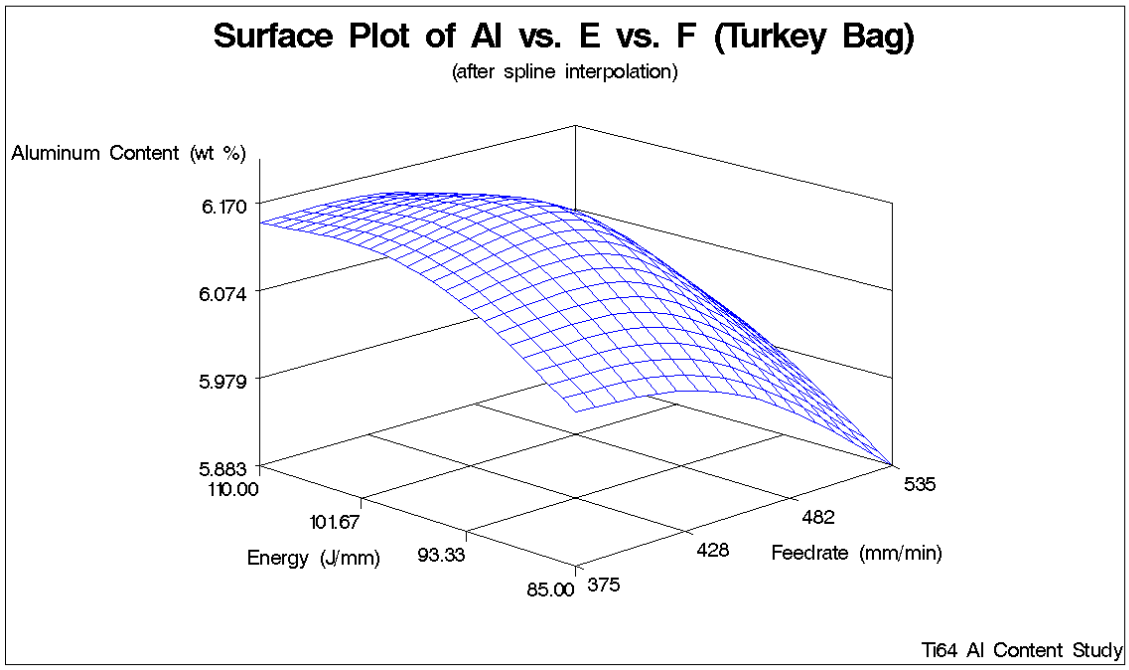

Figure 4.3. Response surface plot of the turkey bag data with default rotation and tilt.

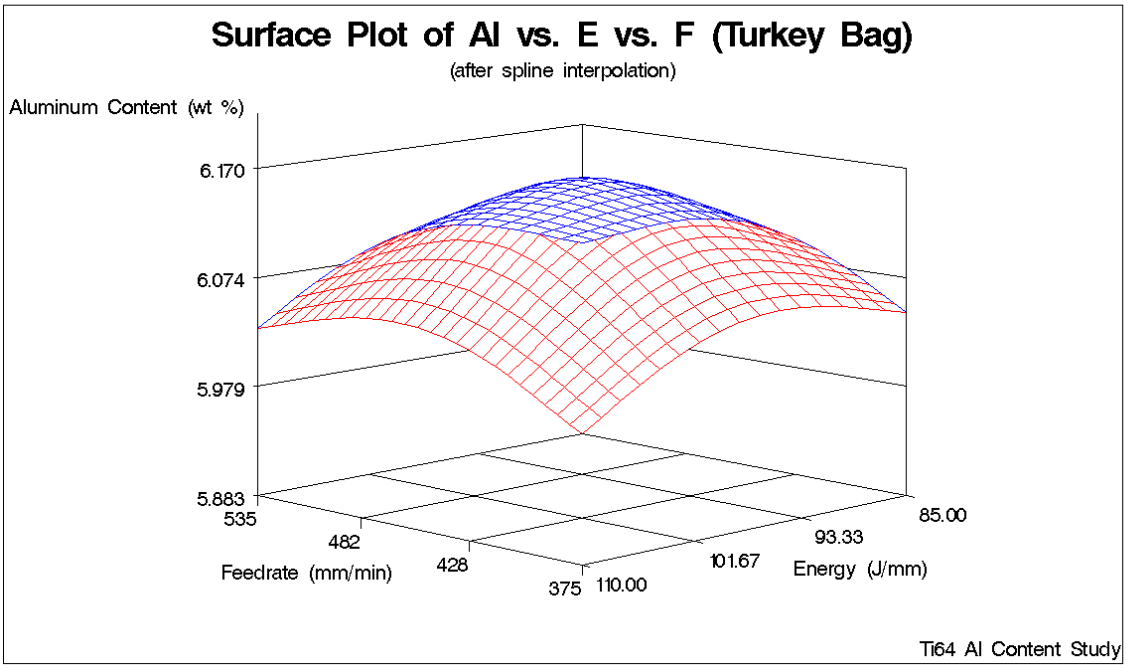

Figure 4.4. Response surface of turkey bag data with 135° rotation and 80° tilt.

Figures 4.5 and 4.6 below, show that optimal parameter sets for the shroud data are slightly less defined than in the overall and turkey bag plots. However, ¼ of the parameter space can be utilized with only ~ 4.4% variation in aluminum content. Therefore, consistent deposits could still be produced based on this model.

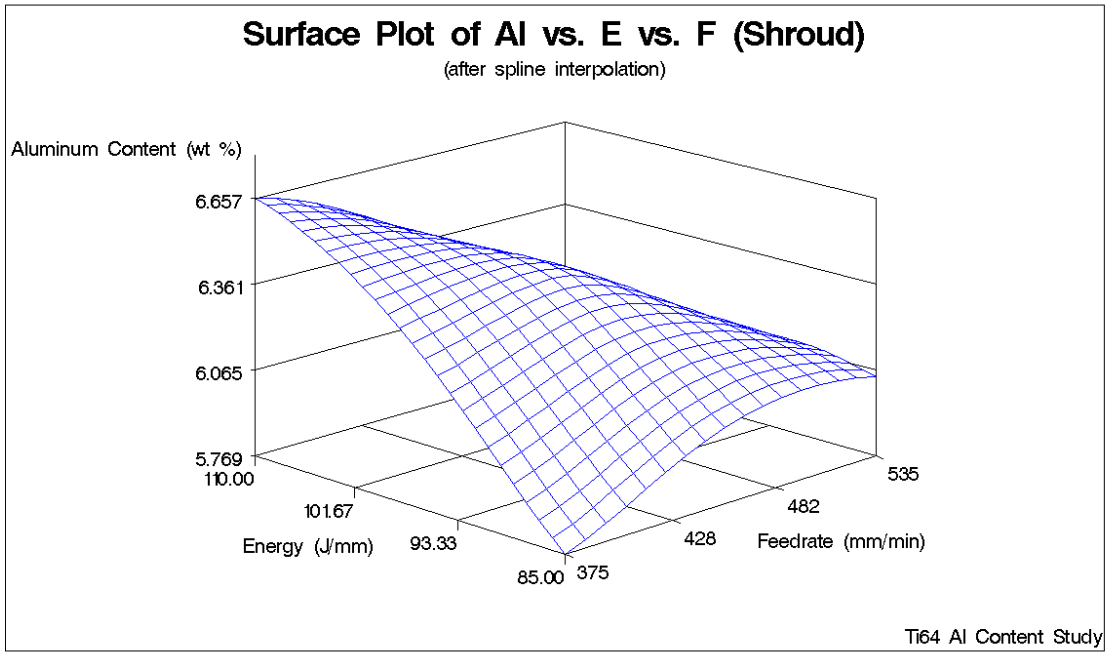

Figure 4.5. Response surface for the shroud data set with default rotation and tilt.

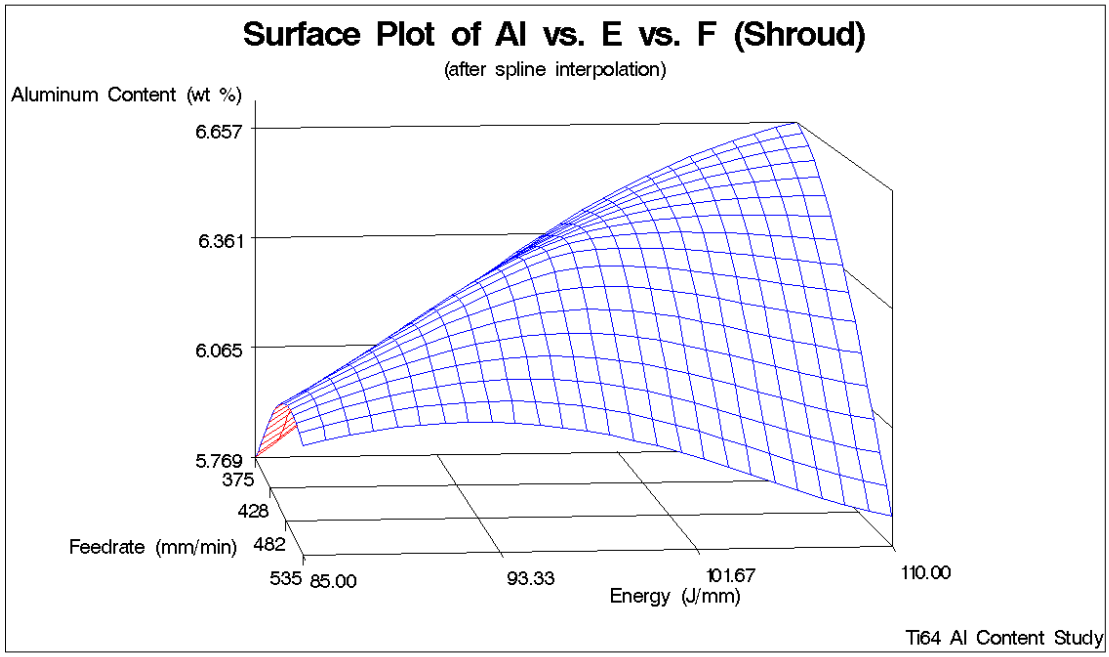

Figure 4.6. Response surface for the shroud data with 275° rotation and 80° tilt.

All of the response surface plots above depict a very surprising trend. The fact that the aluminum content is highest when the deposition is performed “slow and hot” (low feedrate and high energy) is counter to conventional thinking. As mentioned in section 1.1 and shown in Figure 1.1, as the temperature increases, evaporation rate increases as well. Conventional thinking would dictate that in order to keep the temperature down, one must increase the feedrate proportional to any increase in laser power. The fact that the results seem to indicate otherwise, was unexpected.

One possible explanation for these results lies in the surface-area-to-volume ratio of the melt pool. Research has been done which closely links the ratio to the aluminum content in Ti64 deposits. It has been shown that as the ratio increases, aluminum loss increases as well [3]. This could help to explain the higher aluminum content achieved with the slow and hot parameter setting. By increasing the energy, and lowering the feedrate, a deeper, wider, melt pool is achieved. This increase in melt pool depth and width will cause the volume to increase, thereby decreasing the surface-area-to-volume ratio. This decrease in surface-area-to-volume ratio will cause a decrease in aluminum loss.

Also surprising was the apparent aluminum enrichment of the deposits. Before performing the deposition, Inductively Coupled Plasma mass spectrometry (ICP) analysis was performed on the powder. The ICP analysis reported the weight percent of aluminum in the powder at 6.00%. The results from the EDS analysis of the deposits indicated aluminum levels reaching as high as 7.17%. While this could be the result of error during the EDS analysis, another possible explanation is aluminum enrichment. The enrichment could be caused by the oxidation of titanium and possibly vanadium. This oxidation

could cause the amount of titanium and/or vanadium in the deposit to decrease, thereby increasing the amount of aluminum relative to the other two.

As mentioned before, another possibility for the inflated aluminum levels is EDS error. This error could be due to several factors. When performing EDS it is crucial that the analyzed surfaces are completely flat. This is the reasoning for polishing to a mirror finish, and removing all scratches. Even though the coupons were polished to a mirror finish, and no scratches were observed while in the scope, the coupons were still mounted onto stubs and placed into the SEM. The position of the coupons, while mounted to the stubs, likely left them in a position such that they weren't exactly perpendicular to the electron beam and therefore not flat. Additionally, the standard and the coupons all need to be mounted at the exact same height in order to achieve the best results. As the coupons were mounted by hand to pen stubs, which were then mounted in the machine, it is likely that they were not all at the exact same height. This would also affect the results of the EDS analysis. Both of these factors are coupled with the inherent +/- 5% accuracy which is associated with this type of analysis.

ICP analysis was performed on three of the samples (#6, #10, #15) by an outside laboratory. This was done to verify the aluminum levels. The three samples were chosen based upon two main criteria. They were selected such that there was little variation in EDS measurements between the bottom, middle, and top of the deposits. This was done so that a sample wasn't selected which had a large variation in aluminum content between two locations in the deposit. This selection was completed so that a more direct comparison could be made between the average aluminum content found by EDS analysis and the aluminum content found through ICP analysis. The second factor

considered when selecting the coupons to be analyzed was the average aluminum content. It was decided that it would be best to select samples such that one sample would have low aluminum content, one sample would have moderate aluminum content, and one sample would have high aluminum content. It was decided that the moderate and high samples should both be well over 6% aluminum, in order to better verify if aluminum enrichment was occurring.

Table 4.4 shows a comparison between the average EDS results, and the ICP results from the three coupons that had ICP analysis performed on them. As shown below coupon 6 fell just outside the standard error range for EDS with a difference between EDS and ICP of ~5.4%. Coupon 10 fell well within the limits of EDS with a difference of ~1.2%. Coupon 15 fell well outside the normal error limits for EDS with a difference of ~18.2%. All three of the samples were found to have Al levels below 6%. Based upon these results and the inherent error, mentioned previously, associated with performing this type of analysis using EDS, a conclusion can be drawn that the inflated aluminum levels were likely due to EDS error.

Table 4.4. Comparison of EDS and ICP results.

Coupon #	Average EDS Results	ICP Results
6	6.31	5.97
10	5.88	5.95
15	6.81	5.57

The results indicating optimal, slow and hot conditions are not without validation. Dongare [15] found that Ti64 deposits created at conditions nearly identical to the slow and hot conditions presented here, yielded deposits of higher strength than deposits created with other parameter sets. Further, it has been found that increased aluminum content considerably increases the strength of titanium, and at levels below 7% Al, titanium alloys maintain good plasticity [16]. This would seem to suggest that the higher strength found by Dongare could be the result of higher Al content. The slow and hot conditions used here were nearly identical to conditions used by Dongare which produced the highest strength deposits.

Additional analysis of the three coupons that were sent out for ICP analysis was completed in order to see how well the ICP results matched up with the model predicted results for aluminum content. Table 4.5 lists the model predicted aluminum content and the aluminum content measured from the ICP analysis for coupons 6, 10, and 15. Coupons 6 & 10 were both produced with the parameter set consisting of low energy and high feedrate. The model predicted aluminum levels for coupons 6 & 10 do match up with the ICP results, with an error of approximately 1.2%. The model predicted result for coupon 15 however, does not match up well with the ICP results. The approximate error between model predicted results and ICP results for coupon 15 was 15%. Coupon 15 was produced with the parameter settings consisting of high power and low feedrate, or ‘slow and hot’ conditions.

The ICP results have shown that two of the coupons have aluminum levels that match up well with the model, and that one does not. Further, since the surprising result drawn from this work was that the slow and hot conditions yielded deposits of higher

aluminum content and the ICP results indicate otherwise casts some doubt over the findings. However, ICP analysis was performed on only one of four coupons that were produced using the slow and hot conditions. Therefore, the ICP results can not completely in-substantiate the model, but they do draw into question the model's validity. In order to further validate or in-substantiate the model, further ICP analysis should be done to gain a larger data set by which to make a more informed conclusion.

Table 4.5. Comparison of model predictions and ICP results.

Coupon #	Model Predicted Results	ICP Results
6	5.90%	5.97%
10	5.90%	5.95%
15	6.40%	5.57%

5. CONCLUSIONS

An experiment was designed, performed, and analyzed in order to establish an optimal set of process parameters. This optimal parameter set will allow consistent chemical composition across Ti-6Al-4V deposits.

- The experimental method produced data with a high level of statistical significance.
- The statistical analysis showed that the interaction effect between energy and feedrate was extremely significant.
- Because of the interaction significance, both energy and feedrate effects were significant.
- There is no statistically significant difference between deposition in a turkey bag and deposition with a shroud on final aluminum content.
- There is no statistically significant difference in aluminum content between the bottom, middle, and top of the deposits.
- Maintaining Energy levels between 97.5 J/mm – 110 J/mm, and Feedrate levels between 375 mm/min – 455 mm/min, should allow for Ti64 deposits of consistent aluminum content.
- Further ICP analysis should be completed on more of the coupons, to better verify the model.

APPENDIX

Table A.1. Raw data obtained from the EDS analysis.

Sample		Al	Ti	V	Fe		Height (in)	Length (in)	Width (in)
1B	1	REPLACED WITH # 21							
1M	2								
1T	3								
2B	1	7.17	90.09	2.26	0.48		0.82	1.1	0.232
2B-2	1	6.27	78.99	2.01	0.46				
2M	2	6.19	78.53	1.9	0.31				
2T	3	6.17	77.83	1.97	0.33				
3B	1	5.84	86.63	6.37	0.11		0.74	1.1	0.262
3B-2	1	5.6	87.97	6.86	0.1				
3M	2	6.32	90.79	4.59	-0.12				
3T	3	5.05	91.08	-6.63	0.07				
3T-2	3	2.61	88.65	-11.54	0.11				
4B	1	6.43	90.89	1.17	-0.02		0.79	1.099	0.234
4M	2	6.15	86.94	5.77	0.14				
4T	3	5.89	83.65	2.41	0.12				
5B	1	6	87.95	6.72	0.28		0.573	1.118	0.269
5M	2	6.19	88.46	4.02	0.26				
5T	3	6.07	90.55	2.51	0.009				
6B	1	6.33	90.76	4.12	0.3		0.757	1.096	0.235
6M	2	6.29	90.19	4.55	0.28				
6T	3	6.32	90.15	4.48	0.33				
7B	1	6.09	89.37	4.23	0.31		0.787	1.088	0.199
7B-2	1	5.64	83.69	3.91	0.18				
7B-3	1	5.63	83.46	4.2	0.24				
7M	2	5.95	86.3	4.38	0.25				
7M-2	2	5.9	85.69	4.16	0.24				
7T	3	6.06	88.3	4.4	0.23				
7T-2	3	5.96	87.77	4.31	0.27				
8B	1	6.31	90.97	4.29	0.25		0.712	1.109	0.26
8M	2	6.34	90.8	4.7	0.35				
8T	3	6.42	90.92	4.71	0.34				
9B	1	6.25	86.67	4.37	0.22		0.779	1.089	0.196
9M	2	6.18	85.99	4.21	0.21				
9T	3	6.16	85.61	4.18	0.001				
10B	1	5.81	87.01	3.94	0.32		0.74	1.1	0.227

10M	2	5.92	87.92	4.49	0.27				
10T	3	5.92	88.11	4.57	0.25				
11B	1	5.99	85.22	3.7	0.24		0.679	1.098	0.226
11M	2	6.15	87.76	3.89	0.27				
11M-2	2	6.23	87.82	3.78	0.31				
11T	3	6.4	91.24	3.96	0.34				
12B	1	6.74	91.81	3.95	0.3		0.633	1.1	0.235
12M	2	6.66	92.68	4.02	0.33				
12M-2	2	6.65	91.17	3.92	0.33				
12T	3	5.98	88.19	4.1	0.35				
13B	1	5.94	86.89	4.51	0.28		0.591	1.109	0.264
13M	2	6.15	89.25	4.46	0.25				
13T	3	6.03	90.3	4.66	0.28				
14B	1	6.61	93.53	4.03	0.37		0.562	1.081	0.212
14M	2	6.55	91.86	4.03	0.33				
14T	3	6.69	93.78	3.91	0.45				
15B	1	6.9	94.89	3.77	0.26		0.551	1.114	0.241
15M	2	6.74	92.13	4.06	0.35				
15T	3	6.78	92.72	3.95	0.37				
16B	1	6.24	86.36	4.25	0.22		0.501	1.096	0.224
16M	2	6.15	84.02	4.18	0.16				
16T	3	6.13	84.81	3.66	0.26				
17B	1	5.79	76.37	1.71	0.18		0.536	1.092	0.198
17M	2	5.78	76.23	1.84	0.2				
17T	3	6.16	86.73	4.24	0.18				
18B	1	REPLACED WITH # 22							
18M	2								
18T	3								
19B	1	5.51	82.65	3.8	0.22		0.667	1.091	0.198
19B-2	1	5.54	82.44	3.68	0.22		0.667	1.091	0.198
19M	2	5.65	83.7	4.14	0.18				
19T	3	5.81	86.82	3.57	0.14				
20B	1	5.85	77.19	1.72	0.15		0.686	1.104	0.222
20M	2	5.93	78.1	1.86	0.15				
20T	3	5.94	78.56	1.92	0.19				
21B	1	6.57	93.3	4	0.4		0.775	1.1	0.25
21M	2	6.55	92.58	4.01	0.58				
21T	3	6.68	95.46	3.62	0.53				
22B	1	5.45	73.99	1.72	0.16		0.672	1.1	0.253
22M	2	5.64	76.98	1.87	0.12				
22T	3	5.85	78.56	1.87	0.2				

Totals		425.84	6084.77	238.95	17.33				
		Al	Ti	V	Fe				
Average		6.08	86.93	3.41	0.248				

REFERENCES

[1] J. Ruan, T. E. Sparks, Z. Fan, J. K. Stroble, A. Panackal, F. Liou, "A Review of Layer Based Manufacturing Processes for Metals," Department of Mechanical and Aerospace Engineering, Missouri University of Science and Technology (formerly University of Missouri – Rolla), Proceedings of the 17th Annual SFF Symposium, Austin, TX, pp. 233-245 (2006).

[2] Yaxin Bao, "Mechanical Properties and Microstructure Study for Direct Metal Deposition of Titanium Alloy and Tool Steel", A Thesis, Missouri University of Science and Technology (formerly University of Missouri-Rolla) (2007).

[3] C. A. Brice, B. T. Rosenberger, S. N. Sankaran, K. M. Taminger, B. Woods, R. Nasserrafi, "Chemistry Control in Electron Beam Deposited Titanium Alloys," Materials Science Forum, Volumes 618-619, pp. 155-158, (2009).

[4] E. Huerta, V. Popovski, "A Study of Hold Time, Fade Effects and Microstructure in Ductile Iron," Proceedings of the AFS Cast Iron Inoculation Conference, Schaumburg, Illinois, pp. 43-56, (2005).

[5] J.A. Taylor, M.J. Cooper, C.L. Smith, D.P.K. Singh, "Dissolution, Recovery and Fade of SR Master Alloys in Al-7SI-0.5MG Casting Alloy," The Minerals, Metals, and Materials Society, Journal of Light Metals, pp.1095-1100, (2005).

[6] J.F. Lancaster, "The Physics of Welding," Journal of Physics Technology, Vol. 15, pp. 73-79, (1984).

[7] RE. Honig, D.A. Kramer, "Vapor Pressure Data for the Solid and Liquid Elements," RCA Rev 1969:30:285,(1969).

[8] Technical Data, Jefferson Lab, url: http://education.jlab.org/itselemental/ele023.html, date accessed: 03/01/2013.

[9] Technical Data, Jefferson Lab, url: http://education.jlab.org/itselemental/ele022.html, date accessed: 03/01/2013.

[10] Titanium Ti-6Al-4V (Grade 5), STA, ASM, Aerospace Specification Metals, Inc. url: http://asm.matweb.com/search/SpecificMaterial.asp?bassnum=MTP642, date accessed: 02/07/2013.

[11] V.G. Ivanchenko, O.M. Ivasishin, S.L. Semiatin, "Evaluation of Evaporation Losses during Electron-Beam Melting of Ti-Al-V Alloys," Metallurgical and Materials Transactions B, Volume 34, Issue 6, pp 911-915, (2003).

[12] T. Fu, Z. Fan, S. Pulugurtha, T. Sparks, J. Ruan, F. Liou, J. Newkirk, "Microstructural Characterization of Diode Laser Deposited Ti-6Al-4V," Missouri University of Science and Technology, Proceedings of the 19th Annual SFF Symposium, Austin, Tx., pp110-115, (2008) .

[13] D. Montgomery, "Design and Analysis of Experiments," 8th ed., John Wiley & Sons, pp. 1-20, (2012).

[14] S. Dongare, "Development of a Technique for Testing of Tensile Properties with Miniature Size Specimens for Metal Additive Manufacturing," A Thesis, Missouri University of Science and Technology, (2012).

[15] L. S. Moroz, I. N. Razuvayeva, S. S. Ushkov, "Characteristics of the Effect of Aluminum on the Mechanical Properties of Titanium," NASA Technical Translation, url: ia600501.us.archive.org/21/items/nasa_techdoc_19740022890/19740022890.pdf, date accessed: 03/11/2013.

VITA

The author, Richard Charles Barclay, was born in Independence, Missouri. He attended high school at William Chrisman High School in Independence. After high school Mr. Barclay spent 10 years working full time in the manufacturing industry, with most of that time spent at A-Z Manufacturing & Sales, located in Independence, Missouri. Mr. Barclay went on to complete his B. S. in Mechanical Engineering with an emphasis in Manufacturing Processes and a minor in Business at Missouri S&T in 2012, graduating Magna Cum Laude. During his time as an undergraduate Mr. Barclay worked for the Manufacturing Engineering Department as an Undergraduate Research Assistant, working on projects for companies such as GKN Aerospace and Boeing Research and Technology. His work with Boeing garnered him an invitation to attend DARPA meetings at Camp Pendleton, CA, on two separate occasions to present the work that his team had completed.

In July of 2012, Mr. Barclay joined the Master of Science in Manufacturing Engineering program at Missouri S&T. He also took a position with the Department as a Graduate Research Assistant. Mr. Barclay's research interests lie in the field of manufacturing process development. At Missouri S&T his work was focused on Laser Metal Deposition. Mr. Barclay was awarded his M. S. in Manufacturing Engineering on May 17, 2013.